ELSEVIER

Applied Surface Science 171 (2001) 213–225

applied surface science

www.elsevier.nl/locate/apsusc

Analytical evaluation of tapping mode atomic force microscopy for chemical imaging of surfaces

Bernhard Basnar[a], Gernot Friedbacher[a,*], Helmut Brunner[b], Thomas Vallant[b], Ulrich Mayer[b], Helmuth Hoffmann[b]

[a]Institute of Analytical Chemistry, Vienna University of Technology, Getreidemarkt 9/151, A-1060 Wien, Austria

[b]Institute of Inorganic Chemistry, Vienna University of Technology, Getreidemarkt 9/153, A-1060 Wien, Austria

Received 16 March 2000; accepted 17 August 2000

Abstract

Scanning probe methods like atomic force microscopy (AFM) and related techniques are promising candidates for morphological, physical, and chemical characterization of surfaces on the sub-micrometer scale. In order to evaluate the analytical potential of tapping mode AFM for obtaining material specific information on surface structures along with topography, we have studied the influence of various experimental parameters on height and phase contrast using self-assembled monolayers (SAMs) as well defined model systems. The organic films were deposited onto silicon substrates starting from alkyltrichlorosilanes with methyl-, ester-, and hydroxyl-end groups, respectively. As a result it was found that reproducibility suffers from the fact that even small changes in parameters determining the force interaction between tip and sample can lead to pronounced changes in image contrast. Nevertheless it has been possible to identify comparatively stable regions for the imaging parameters allowing to distinguish different sample systems by their specific pattern of height and phase contrasts, which can be seen as a valuable analytical contribution towards sub-micrometer chemical imaging with scanning probe microscopy. © 2001 Elsevier Science B.V. All rights reserved.

PACS: 61.16.Ch; 68.60.Bs; 81.70.Jb; 81.15.Lm

Keywords: Atomic force microscopy; Phase detection imaging; Self-assembled monolayers; Chemical imaging; Elasticity

1. Introduction

In many research areas the possibility of analyzing surface properties with high resolution down to the atomic or molecular level is becoming increasingly important. Atomic force microscopy (AFM) is one of the most powerful techniques for nanoscopic characterization of surfaces. Usually, obtaining information on the sample's morphology is straightforward, since AFM images primarily contain topographical information. However, in many cases also information on other physical (e.g. elasticity, hardness, tribological behavior) and chemical properties is needed with sub-micrometer resolution. In order to access such properties, a number of different approaches based on the principles of AFM have been pursued.

Friction force microscopy [1–3] has been shown to be able to produce image contrast between surface

* Corresponding author. Tel.: +43-1-58801-15110; fax: +43-1-58801-15199.
E-mail address: gernot.friedbacher@tuwien.ac.at (G. Friedbacher).

0169-4332/01/$ – see front matter © 2001 Elsevier Science B.V. All rights reserved.
PII: S0169-4332(00)00761-3

regions terminated by different functional groups through varying friction between the surface and the AFM tip in contact mode. However, the general applicability of this technique for chemical surface imaging is hampered by the fact that shear induced destruction of surface structures may occur. Moreover, also the surface topography plays an important role in the generation of the friction contrast. Thus, friction images cannot be solely interpreted in terms of chemical interactions between tip and sample surface.

In force modulation AFM [4], the force between the tip and the sample surface is modulated by either vibrating the sample or the cantilever in vertical direction while the tip is raster-scanned across the surface in contact mode. The varying compliance of the sample can be monitored through the responding amplitude signal of the cantilever. In this way a lateral distribution image of the surface hardness can be obtained.

Force–distance curves and load-indentation curves can be utilized to record the force interaction between the sample surface and the AFM tip while approaching the surface to the tip or retracting it again. In such measurements adhesion between the tip and the sample opens up the potential of accessing chemical information on the sample surface. Elastic information can be retrieved by the indentation behavior of the tip. More recently the so-called pulsed force mode (PFM) [5] has been introduced which allows continuous recording of force–distance and load–indentation curves across the whole scan area.

One drawback of the described techniques is the risk of damaging the sample due to high loading forces or lateral shear forces. In this respect tapping mode AFM (TMAFM) [6,7] along with phase detection imaging (PDI) [8,9] is a promising tool for obtaining morphological as well as physical and chemical information under more gentle conditions in intermittent contact mode. In TMAFM height information is delivered by the amplitude signal of the oscillating cantilever. The phase lag between the driving oscillation and the cantilever response is a very sensitive measure for the force interaction between the tip and the sample surface.

In the literature different approaches can be found for discriminating the origin of phase contrast. Bar and coworkers have reported on the influence of different sample and tip properties on the phase contrast both experimentally [10,11] and from a theoretical [12–14] point of view. Their results show the largely harmonic nature of the oscillation and the relationship between energy dissipation and phase contrast. Chen et al. have reported on optimization of phase imaging via dynamic force curves implementing computer simulations in their discussion [15]. An in-depth theoretical study of the cantilever motion as well as the tip-sample interaction was performed by Fuchs and coworkers [16–18], leading to a quantitative description of the oscillating system. Tamayo and Garcìa have investigated the interaction mechanism between tip and sample [19,20] emphasizing the influence of the changes in the oscillation amplitude on interaction time, force, and contact area. The work of Magonov and coworkers [21–23] as well as the work described in [24–26] mainly focuses on the determination of the structure and mechanical properties of polymers, linking higher crystallinity with smaller phase lags. Noy et al. have established a quantitative relationship between the strength of the tip-sample interaction and the phase lag [27].

Apart from tapping mode phase lag investigations, especially LFM has received considerable attention. For instance, Lieber and coworkers have developed the chemical force microscope (CFM), utilizing LFM with chemically modified tips [28–30] for obtaining chemical contrast via friction. This approach has also been pursued by the group of Spencer [31–33]. The publications of these groups emphasize the influence of hydrophilic interaction as the main mechanism for image contrast. The group of Salmeron has used LFM to investigate the influence of the chain length of organic molecules on gold and mica and the influence of the measurement force on friction [34–36]. As a result, it has been shown that friction with short chains is largely induced by disorder effects. Moreover, different friction regimes depending on the tip load and the physico-chemical properties of sample and tip are discussed [37]. Utriainen et al. [38] correlate the friction on inorganic thin film structures to differences in hydrophilicity.

One of the major difficulties in interpreting phase lag images is the variety of influential parameters which can contribute to the signal (e.g. elasticity and viscoelasticity [19,20,39], moisture on the surface [11], surface chemistry [27], instrumental parameters

[20], and cantilever tip quality [40]). To a smaller extent such parameters can even influence the amplitude signal leading to height artefacts in topographical AFM images [10,11,22,41–45].

In this work we have utilized self-assembly of organic monolayers for producing structurally and chemically well-defined model samples for investigation of the influence of various imaging parameters on phase and height contrast for different systems. The analytical approach of this work is a discrimination between chemical and physical properties utilizing SAM structures as well-defined reference samples for calibration of the measurement process.

2. Experimental section

2.1. Sample preparation

Substrates were prepared by carving and breaking Si(1 0 0) wafers into pieces of 1 cm × 1 cm in size. The chemicals used were toluene (Aldrich, 99.8%), ethanol (Austria Hefe AG, 99.8%), acetone (Aldrich 99.9%), tetrahydrofurane (HF) (Aldrich, >99.5%), hydrochloric acid (Fluka, fuming 37%), lithium aluminum hydride ($LiAlH_4$) (Aldrich, 1.0 M in THF), octadecyltrichlorosilane (OTS) (Aldrich, 99.5%), and trichlorosilylheptadecanoic acid methyl ester (TSHME) (synthesized according to [46]).

Table 1 shows the samples used in our studies. These samples have been prepared according to the scheme shown in Fig. 1. In addition to these samples, multilayered structures have been produced for studying elasticity effects. These structures were obtained by repeated deposition and reduction of TSHME on sample 3 (ODS/OH-HDS) until the desired number of layers was reached.

2.2. AFM measurements

All AFM measurements were carried out with a NanoScope III Multimode SPM (Digital Instruments, Santa Barbara, CA) operated in tapping mode. Single crystal Si-cantilevers (Nanosensors, Germany) with resonance frequencies in the order of 300–400 kHz and spring constants between 10 and 40 N/m have been used for the experiments. In addition, also chemically modified tips have been used. These have been prepared by full monolayer coating with ODS according to the scheme shown in Fig. 1 (similar to sample 1, but with a longer adsorption time of approximately 2 h). The AFM was operated under ambient conditions. Both topographic and phase images were recorded at free oscillation amplitudes

Table 1
Overview of the samples under investigation

Sample no.	Sample	Surface composition	Structure	Remarks
1	ODS/Si	ODS[a] islands on Si	Sub-monolayer coverage (stepped surface)	~50% CH_3-terminated surface ~50% oxidized Si surface
2	ODS/TSHME	ODS and TSHME[b] areas	Full monolayer coverage (flat surface)	~50% CH_3-terminated surface ~50% ester-terminated surface
3	ODS/OH-HDS	ODS and OH-HDS[c] areas	Full monolayer coverage (flat surface)	~50% CH_3-terminated surface ~50% OH-terminated surface
4	ODS/2 × ODS	ODS	Full monolayer and double layer islands (stepped surface)	Fully CH_3-terminated surface
5	ODS/2 × TSHME	ODS and TSHME areas	ODS monolayer and TSHME double layer islands (stepped surface)	~50% CH_3-terminated surface ~50% ester-terminated surface

[a] ODS: octadecylsiloxane layer.
[b] TSHME: ester-terminated siloxane layer obtained through deposition of trichlorosilylheptadecanoic acid methyl ester (TSHME). For simplicity of terminology TSHME is also used as abbreviation for the respective siloxane layer throughout the paper.
[c] OH-HDS: OH-terminated heptadecylsiloxane layer (obtained through reduction of TSHME layer).

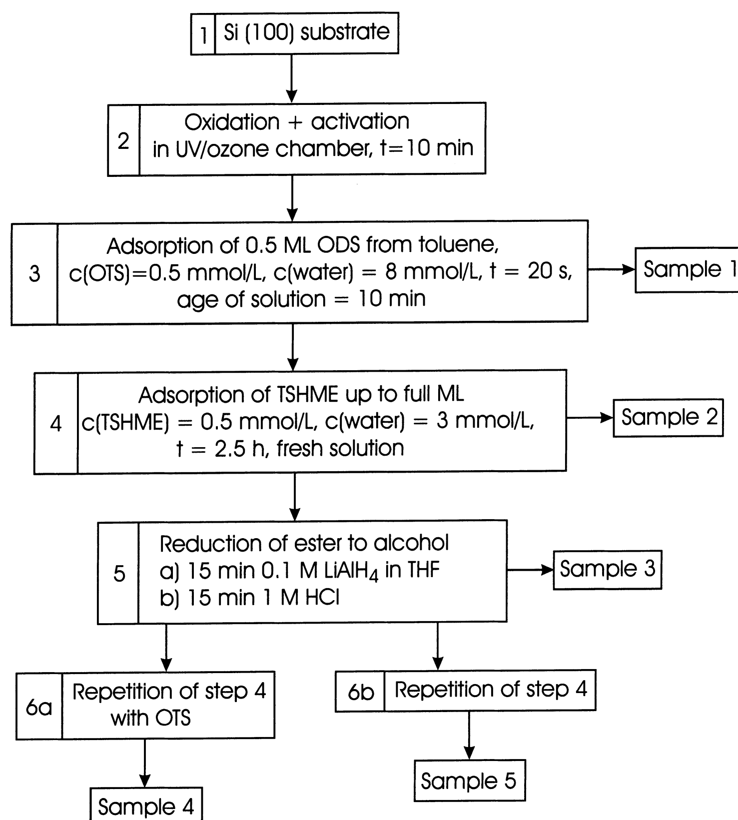

Fig. 1. Scheme of sample preparation. Between the single steps, the samples were rinsed with toluene, acetone, and ethanol, blow-dried with nitrogen and the film thickness was measured ellipsometrically (ML = monolayer).

A_0 of approximately 50, 250, and 400 nm. If not stated otherwise, measurements were performed at a setpoint amplitude A_{sp} of $0.7 \times A_0$ ($r_{sp} = 0.7$). Data analysis was carried out with the NanoScope III software. Both the height and the phase images were evaluated by bearing analysis which yields a histogram of the height or phase shift values in the image, respectively. In this way values for the surface coverage have been calculated from typically five AFM images taken at different sample positions.

2.3. Ellipsometric measurements

The film thickness of the samples was monitored ellipsometrically during sample preparation using an SD 2300 instrument (PLASMOS, Munich, Germany). Experimental details are given elsewhere [46].

3. Results and discussion

In order to analytically utilize phase and height contrasts for chemical characterization of surfaces, first the influence of experimental settings, of the tip, and of sample properties has been investigated.

3.1. Influence of experimental settings

In this chapter results addressing the influence of the most important settings, the free oscillation amplitude A_0 of the cantilever and the damping ratio r_{sp} ($r_{sp} = A_{sp}/A_0$, where A_{sp} is the setpoint amplitude maintained constant during imaging), will be described. Since the experimental results can be more or less influenced also by other parameters like feedback gains or scan direction, it is important to

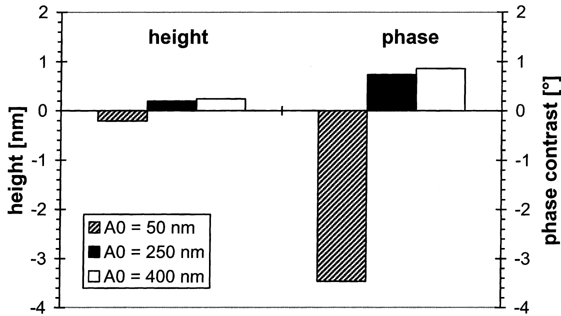

Fig. 2. Height and phase contrast on sample 1 (ODS/Si) measured at $r_{sp} = 0.7$ and different values of A_0. Positive values indicate that the height, respectively, phase lag is larger on the ODS layer.

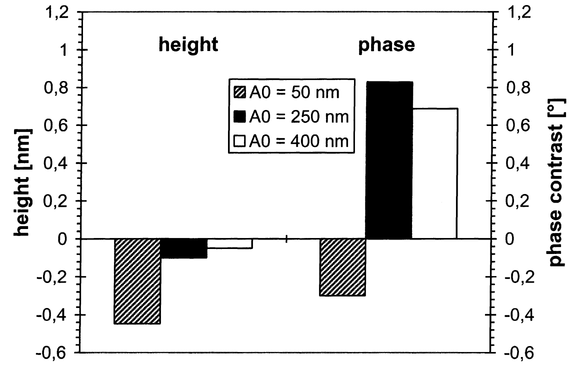

Fig. 3. Height and phase contrast on sample 2 (ODS/TSHME) measured at $r_{sp} = 0.7$ and different values of A_0. Positive values indicate that the height, respectively, phase lag is larger on the ODS layer.

carefully control all measurement parameters and to keep them constant, when the influence of a particular parameter is to be studied.

3.1.1. Influence of the free oscillation amplitude

The free oscillation amplitude A_0 has a large influence on both the height and the phase contrast. The higher A_0, the higher the force that can be exerted onto the sample at a given damping ratio r_{sp}. Moreover, for compliant samples, the interaction area can increase as the tip penetrates into or deforms the sample.

Fig. 2 depicts the height and phase contrasts on sample 1 (ODS islands on silicon) observed for amplitudes of 50, 250, and 400 nm. It can be seen that smaller amplitudes tend to yield higher phase contrast. This can be explained by changes in the interaction time between tip and sample and differences in the interaction force. For large amplitudes the interaction time decreases, i.e. the tip remains in the force field of the sample for a shorter period of time. Fig. 3 shows the corresponding behavior found for sample 2 (ODS mixed with TSHME). Here, in contrast to sample 1, the phase contrast increases with increasing A_0 indicating a different contrast mechanism which will be addressed later. Increasing the amplitude from 50 to 250 nm leads to inversion of the phase contrast for all the samples, as can be clearly seen in Fig. 4, for example.

As shown in Fig. 5b, it can also be observed that small amplitudes ($A_0 = 50$ nm) produce higher phase contrast due to chemical surface properties as compared to differences in elasticity. At $A_0 = 250$ nm the contrast for both properties is similar, whereas for $A_0 = 400$ nm again a higher sensitivity towards chemistry is noticed. These findings can be explained by the interaction time and the energy dissipation into the sample. Small amplitudes lead to higher contrasts caused by differences in chemistry, because the time

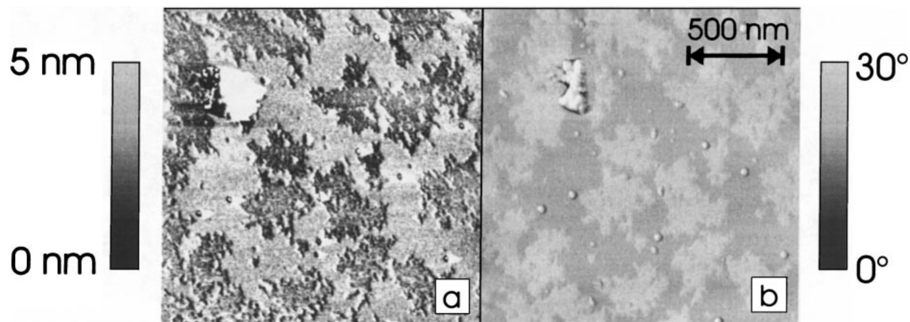

Fig. 4. Phase contrast images of sample 3 (ODS/OH-HDS) recorded at (a) $A_0 = 50$ nm and (b) $A_0 = 250$ nm.

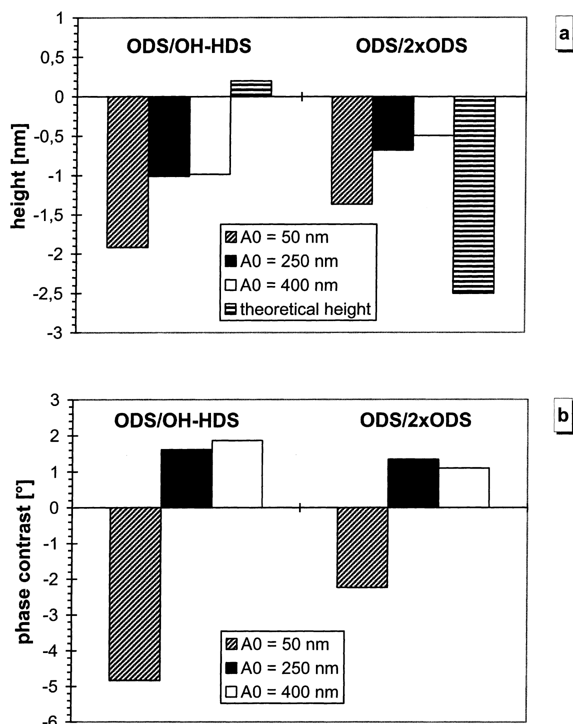

Fig. 5. Comparison of height (a) and phase contrasts (b) for samples 3 (ODS/OH-HDS) and 4 (ODS/2 × ODS).

in the vicinity of the sample surface, and thus also in the short range force field of the sample, is longer than for large amplitudes, favoring a chemical differentiation [13,20,47,48]. For larger amplitudes tip penetration becomes more pronounced favoring elasticity induced contrast. Nevertheless, large amplitudes lead to a pronounced phase contrast on sample 2 (ODS/TSHME) whereas only a small contrast was observed for small amplitudes (see Fig. 3). This might be related to smaller chemical differences between the ODS and the TSHME domains, since the methyl groups of the ester function reduce the possibility for formation of hydrogen bonds between tip and sample, making the behavior of the surface more similar to methyl termination than to carboxyl termination. This is also supported by the contact angles (advancing contact angle with water) of 107, 74, and 20° for methyl, ester, and acid terminal groups, respectively [49]. However, the deformation of the sample leads to an increased contact area and interaction time in softer domains [23,50] inducing a larger phase shift. This is particularly the case for the TSHME terminated regions which, due to a lower degree of order [51], are more compliant [52] than the ODS domains. Furthermore, this behavior might facilitate a stronger interaction of the oxygen groups of the ester function with the hydrophilic tip leading to increased contrast in this particular case.

Fig. 5a shows that the amplitude has a significant influence on the measured height data, too. On sample 4 (ODS/2 × ODS) a pronounced decrease of the step height can be observed with increasing A_0. This can be explained by increasing compression of the layers with increasing interaction forces. On sample 3 (ODS/OH-HDS) a large chemistry induced height artefact is apparent in all cases.

3.1.2. Influence of the damping ratio

Besides the free oscillation amplitude A_0, also the damping ratio r_{sp} (as determined by A_0 and A_{sp}, see above) determines the force being exerted onto the sample. Although the influence of r_{sp} also depends on other parameters like A_0 or the tip quality, in general, a decrease of r_{sp} leads to an increase in the phase contrast (see Fig. 6). It can be observed that the increase of the phase contrast with increasing damping is not steady, but shows a comparatively stable region for low damping ($r_{sp} > 0.65$). With respect to analytical perspectives, this is an important observation, showing that measurements must be performed with settings in such stable regions in order to obtain reproducible results largely unaffected from drifts

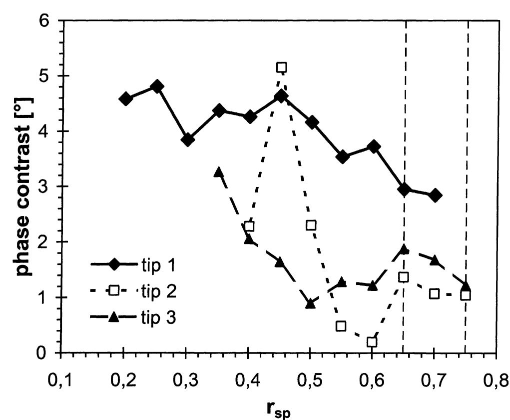

Fig. 6. Phase contrast vs. damping ratio r_{sp} on sample 1 (ODS/Si) measured at $A_0 = 50$ nm with different individual tips (untreated). The vertical lines denote a region in which the phase contrast is comparatively insensitive towards slight changes of r_{sp}.

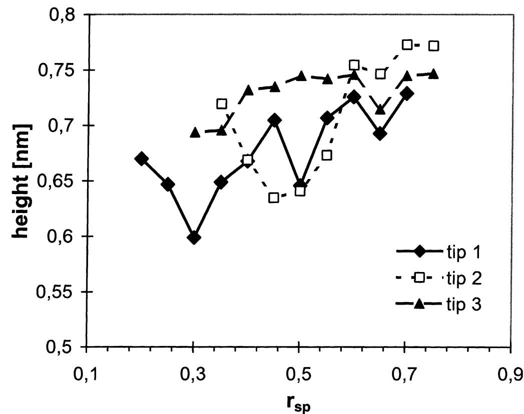

Fig. 7. Height contrast vs. damping ratio r_{sp} on sample 1 (ODS/Si) measured at $A_0 = 50$ nm for different individual tips (untreated).

of the set parameters during measurement. It must be noted, however, that the observed contrast values can differ significantly from tip to tip as can be seen in Fig. 6. Thus, they can only be seen as a means for determining sample properties with appropriate reference measurements on known materials. It has also been observed that bad tips (like tip 2 in Fig. 6), leading to blurred artefacteous images, show a different response of the phase angle with changes in the damping. Since cleaning of such tips in a UV/ozone chamber leads to improved image quality again, the observed artefact is most likely due to contamination of the tip.

In the height measurements, the damping ratio shows an insignificant influence compared to other parameters. Small variations of r_{sp} lead to negligible changes in the height values. Only large variations, especially when working with bad tips, can lead to an observable change in the height contrast (Fig. 7). In general, a slight decrease in the height can be observed with increasing damping, which is probably caused by compression. However, besides compression, as already mentioned for A_0, a higher damping can also effect chemical interactions (e.g. on sample 2-ODS/TSHME, Fig. 5a) influencing the height contrast as well.

3.2. Influence of the tip

One of the most critical parameters affecting image contrast, particularly phase contrast, is the quality of the tip. It has been observed repeatedly that contrast changes can occur spontaneously and also in a reversible manner, which is most probably due to pick-up and loss of impurities during imaging (Fig. 8). Such contrast variations can also proceed gradually with time, which could be explained by a change in the tip shape (stumping by abrasion or contamination) due to mechanical interaction with the sample surface. However, not only the tip shape but also chemical alterations of the tip surface due to adsorption can be associated with the described phenomena. In order to minimize these effects, the interaction force during measurement should be kept as low as possible. Furthermore, when comparing and interpreting image contrasts, prior study of the time dependence of the contrasts on the samples under investigation is necessary. The stability of all relevant measurement parameters can be checked by re-measuring the first sample after a series of specimens.

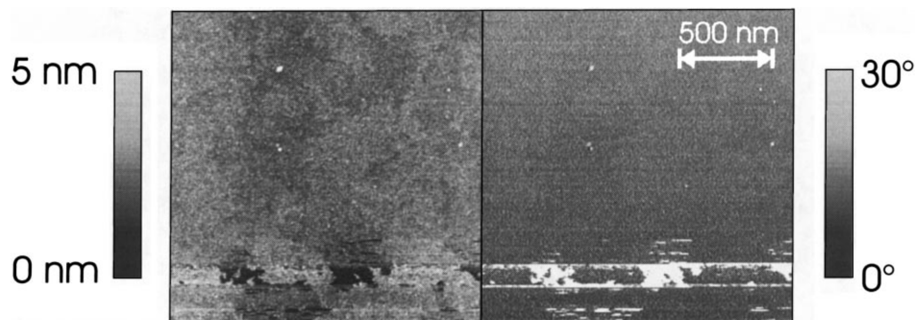

Fig. 8. TMAFM image of sample 2 (ODS/TSHME). At the bottom a spontaneous reversible change of the contrast can be observed. Left: height image, right: phase contrast image.

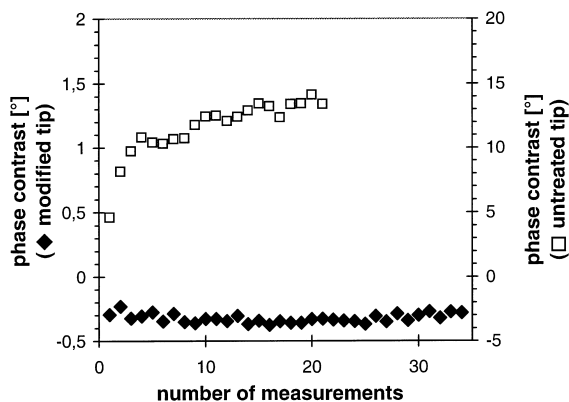

Fig. 9. Long term stability of the phase contrast for an untreated (data taken on sample 4) and a modified tip (data taken on sample 3) over a period of approximately 2 and 3 h, respectively. The time interval between the data points is 5 min. Measurements have been performed at $A_0 = 50$ nm.

Another important aspect with respect to influencing image contrast with the tip are chemical surface modifications of the tip. In our studies we have produced chemically modified tips through full monolayer coverage with ODS. For these modified tips a better long-term stability has been observed compared to untreated commercial silicon single crystal tips. Fig. 9 shows the course of the phase contrasts obtained both with a modified tip (35 measurements) and an untreated tip (21 measurements) over a period of approximately 3 and 2 h, respectively. The increased stability of the modified tips might be explained by a lower susceptibility towards adsorption of impurities and lower wear due to decreased attractive force interaction with the sample. Besides this benefit of modified tips, it must be noted, however, that they should only be operated at low damping ratios ($0.6 < r_{sp} < 0.8$). At smaller r_{sp} frequently a strong increase of the phase contrast is found even for small variations of r_{sp}, making reproducible measurements difficult. This different sensitivity against changes in the damping, and thus the interaction force, might be due to random interlacing of the organic chains of the tip with those of the sample.

3.3. Influence of the sample properties

3.3.1. Influence of the surface chemistry

The chemical termination of the sample surface influences both height and phase contrast due to varying associated long range (e.g. electrostatic) and short range (e.g. chemical bond formation) forces effecting the oscillation of the cantilever. Chemical contrast can either be achieved by (i) direct interaction of functional groups on the tip with those on the sample surface (e.g. hydrophilic/hydrophilic or hydrophilic/hydrophobic interactions or (ii) mediated interaction through liquid neck formation between tip and sample depending on the presence of adsorptive water layers controlled by the hydrophilicity of the surfaces and the surrounding humidity [9,53,54]. In order to exclude erroneous interpretation of results caused by random variation of the humidity of the surrounding environment, only data obtained within individual series taken at constant humidity have been compared directly.

In order to study the influence of the surface chemistry free from elasticity effects, sample 3 (ODS/OH-HDS) has been used as model system. Fig. 10 shows AFM images of this specimen recorded

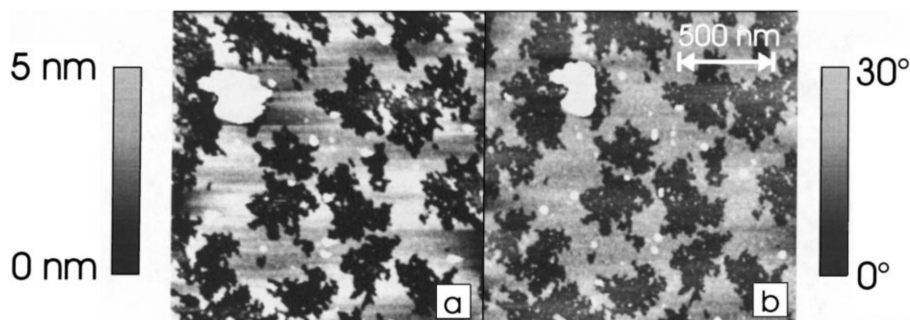

Fig. 10. TMAFM height images of sample 3 (ODS/OH-HDS) recorded at (a) $A_0 = 50$ nm and (b) $A_0 = 250$ nm.

at A_0 of 50 and 250 nm, respectively. For both cases a pronounced height contrast can be observed, although the sample is almost completely flat (see Table 1). For $A_0 = 50$ nm (Fig. 10a) this height artefact is about 18 Å (the OH-HDS regions appear to be elevated), which is even larger than the measured height of one monolayer (see Fig. 5). For larger A_0 (Fig. 10b) this artefact is less pronounced (~10 Å). In comparison, the height artefact on sample 2 (ODS/TSHME) is much lower (see Fig. 3). In fact, for $A_0 = 50$ nm a weak height contrast of ~4 Å (TSHME region slightly elevated) can be seen and for $A_0 = 250$ and 400 nm such a contrast is nearly undetectable anymore. According to the chain length of the film molecules, the ODS layer should by elevated by 2 Å. The different behavior of sample 2 and 3 with respect to this height artefact is in full accordance with expectation, given the fact that the chemical differences in surface termination are much smaller on sample 2.

The strongest height artefact can be observed on sample 1 (ODS/Si). For $A_0 = 400$ nm a height contrast of 2.5 Å is obtained, which is only about 10% of the expected height of one ODS monolayer (26.2 Å, [49]). At this point it should be noted that such erroneous values have already been reported in the literature [55,56] and have so far been mainly ascribed to the compression of the organic layer [57]. For $A_0 = 50$ nm, the height measured by AFM drops to zero and even reversed contrast can occur. This indicates that these artefacteous results are not solely caused by a mechanical deformation and that there is a strong influence of the surface chemistry.

Pronounced phase contrast can be observed for all samples with large differences in chemical composition between the different surface domains. Both for small and for large amplitudes, sample 3 (ODS/OH-HDS) shows the highest contrast. On sample 2 (ODS/TSHME) there is only a very weak contrast for small amplitudes, which can be explained by the similar surface termination on both surface regions as already discussed before. For large values of A_0 a strong increase of the chemical contrast can be observed. As already addressed earlier, a possible explanation for this phenomenon is an increased interaction with the oxygen containing part of the ester group when the hydrophobic methyl groups are pushed aside upon higher interaction forces.

3.3.2. Influence of the elasticity of the sample

The sample's elasticity can cause height artefacts due to different compressibility of the organic layers and the stiffer substrate. Furthermore, compliance of elastic surface regions leads to larger contact areas between tip and sample also controlling chemical interactions which in turn are another source for height artefacts as already mentioned before.

In order to study the role of the elasticity free from surface chemical contributions, multilayered systems of various thickness and nearly uniform surface termination across the whole sample (ODS monolayer and multilayered TSHME structures) have been used as model samples. Generally, it can be observed that the height measured by AFM is always smaller than the nominal thickness of the multilayer domains. For a small number of layers (up to four) the deviation between measurement and expectation is about 50% when measuring at $A_0 = 50$ nm (Fig. 11). For larger A_0 (i.e. higher interaction force at constant r_{sp}) the deviation is greater (up to 75% for $A_0 = 400$ nm) which is an indication for higher compression of the organic chains upon increased interaction forces. For a larger number of layers (more than four) the absolute deviation from the nominal value is constant (~7 nm for $A_0 = 50$ nm) indicating that this deviation is determined by the compliance of surface near zones. Therefore, the relative error in the height

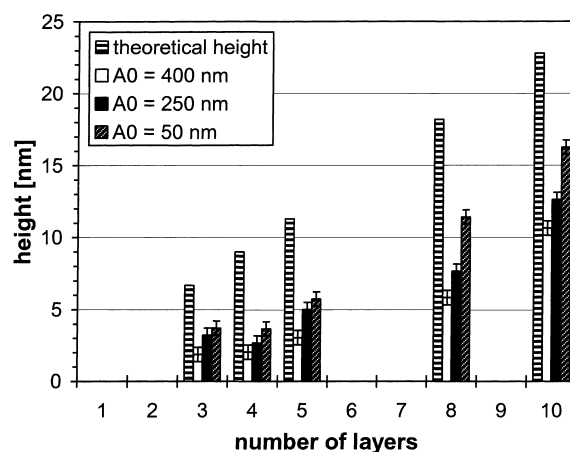

Fig. 11. Measured height values vs. number of layers as determined on multilayered SAM structures. The theoretical heights are shown as well. The data have been recorded with untreated tips at $r_{sp} = 0.7$ and different values of A_0 as shown in the graph.

measurements becomes lower with increasing thickness of the whole multilayer system. These observations illustrate that correct height measurements on the molecular scale are not just a matter of proper piezo calibration. In this region rather "internal" calibration with reference samples of similar properties should be performed in order to take into account various sources of artefacts.

As far as the phase signal is concerned, an increasing phase lag should be observed for increasing energy dissipation from the cantilever into the sample [58]. Such a possibility for increasing energy dissipation is given for layer thickness showing a constant relative height error (up to four layers, as described above). For thicker systems the absolute height deviation due to the sample's compliance is constant. Since the properties of surface near zones, which are relevant for signal generation, are expected to be independent from the layer thickness once a certain total thickness is exceeded, the phase contrast should not change anymore. Although such a trend could be observed in the phase images, large scattering of the phase contrast values did not allow to confirm this conclusion on a quantitative basis.

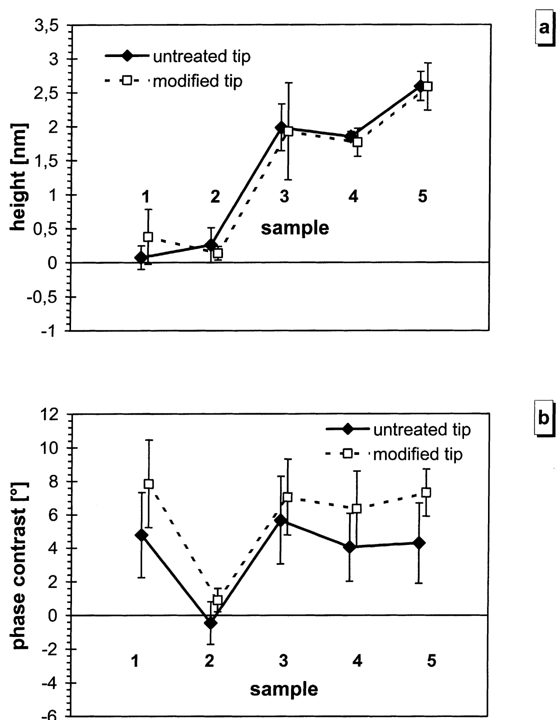

Fig. 12. (a) Height and (b) phase contrasts for various samples under investigation. The data were recorded at $A_0 = 50$ nm and $r_{sp} = 0.7$. It should be noted that fairly large scattering is observed, since raw data obtained with different individual cantilevers over a longer period of time have been implemented. Positive values indicate that the height, respectively, phase lag is smaller on the ODS layer.

3.4. Discrimination of sample systems and properties

Finally, it has been tried to distinguish different sample systems by their height and phase contrasts in the respective AFM images. Fig. 12 shows the results obtained for $A_0 = 50$ nm and $r_{sp} = 0.7$ both for untreated silicon tips and tips modified by coating with ODS. For sake of optimum reproducibility all measurement parameters were kept as constant as possible at the following values: integral gain = 0.3, proportional gain = 3, scan rate = 1 Hz (scan direction from top to bottom, line direction = trace), scan size = 2 μm, resolution = 256 pixel× 256 pixel. Since measurements have been performed on different days and with different tips, the error bars are rather large, especially for the phase contrast. Nevertheless, except for the discrimination between sample 3 and 4, all systems can be distinguished from each other by their pattern of phase and height contrasts at the given settings.

4. Conclusions

Thin layers produced by self-assembly of organic molecules have proven to be valuable model systems for systematically studying the influence of various parameters on height and phase contrast in tapping mode AFM images. Since both layer thickness and chemical surface termination can be controlled independently from each other, the role of mechanical and chemical sample properties can be examined. This opens up the potential for optimizing measurement parameters like free oscillation amplitude A_0 and damping ratio r_{sp} towards maximum sensitivity for the material property of interest. Moreover, the results indicate that stable regions of A_0 and r_{sp} can be identified, where the achieved contrasts are comparatively insensitive towards small drifts of these parameters. Therefore, measurements must be performed

by setting these values within those regions in order to increase reproducibility. Furthermore, it has been found that long-term stability of the experiments can be increased using chemically modified tips coated with an octadecylsiloxane layer. Finally, we have been able to distinguish different sample systems by their pattern of height and phase contrasts. Up to now the general applicability of this concept is limited by data scattering mainly originating from the use of different individual tips. As a first step towards chemical imaging with AFM, this problem may be overcome by checking the performance of individual tips by means of calibration samples produced by self-assembly. Moreover, discrimination of different samples could be facilitated through implementation of height and phase contrast patterns obtained for different instrumental settings like A_0 and r_{sp}. Further improvements could be achieved by more uniform properties of the AFM tips and by better understanding the role of the humidity during measurement which is currently being investigated.

Acknowledgements

Financial support of this work by the Austrian Ministry for Education, Science and Culture and the Austrian Science Foundation (P9065 and P11015) is gratefully acknowledged.

References

[1] J.M. Williams, T. Han, T.P. Beebe Jr., Determination of single-bond forces from contact force variances in atomic force microscopy, Langmuir 12 (1996) 1291–1295.

[2] S.K. Sinniah, A.B. Steel, C.J. Miller, J.E. Reutt-Robey, Solvent exclusion and chemical contrast in scanning force microscopy, J. Am. Chem. Soc. 118 (1996) 8925–8931.

[3] A. Noy, D.V. Vezenov, L.F. Rozsnyai, C.M. Lieber, Force titrations and ionization state sensitive imaging of functional groups in aqueous solutions by chemical force microscopy, J. Am. Chem. Soc. 119 (1997) 2006–2015.

[4] F.-B. Li, G.E. Thompson, R.C. Newman, Force modulation atomic force microscopy: background, development, and application to electrodeposited cerium oxide films, Appl. Surf. Sci. 126 (1998) 21–33.

[5] H.-U. Krotil, T. Stifter, H. Waschipky, K. Weishaupt, S. Hild, O. Marti, Pulsed force mode: a new method for the investigation of surface properties, Surf. Interface Anal. 27 (1999) 336–340.

[6] C. Prater, AC methods in atomic force microscopy, Microbeam Anal. 2 (1993) S57–S58.

[7] Q. Zhong, D. Inniss, K. Kjoller, V.B. Elings, Fractured polymer/silica fiber surface studied by tapping mode atomic force microscope, Surf. Sci. Lett. 290 (1993) L688–L692.

[8] J. Thornton, Tapping-probe phase imaging increases atomic force microscope contrast, Laser Focus World 32/7 (1996) 141–142.

[9] I. Schmitz, M. Schreiner, G. Friedbacher, M. Grasserbauer, Phase imaging as an extension to tapping mode AFM for the identification of material properties on humidity-sensitive surfaces, Appl. Surf. Sci. 115 (1997) 190–198.

[10] G. Bar, Y. Thomann, R. Brandsch, H.-J. Cantow, Factors affecting the height and phase images in tapping mode atomic force microscopy. Study of phase-separated polymer blends of poly(ethene-co-styrene) and poly(2,6-dimethyl-1,4-phenylene oxide), Langmuir 13 (1997) 3807–3812.

[11] R. Brandsch, G. Bar, M.-H. Whangbo, On the factors affecting the contrast of height and phase images in tapping mode atomic force microscopy, Langmuir 13 (1997) 6349–6353.

[12] G. Bar, R. Brandsch, M.-H. Whangbo, Description of the frequency dependence of the amplitude and phase angle of a silicon cantilever tapping on a silicon substrate by harmonic approximation, Surf. Sci. 411 (1998) L802–L809.

[13] G. Bar, R. Brandsch, M. Bruch, L. Delineau, M.-H. Whangbo, Examination of the relationship between phase shift and energy dissipation in tapping mode atomic force microscopy by frequency-sweep and force-probe measurements, Surf. Sci. Lett. 444 (2000) L11–L16.

[14] M.-H. Whangbo, G. Bar, R. Brandsch, Description of phase imaging in tapping mode atomic force microscopy by harmonic approximation, Surf. Sci. 411 (1998) L794–L801.

[15] X. Chen, M.C. Davies, C.J. Roberts, S.J.B. Tendler, P.M. Williams, N.A. Burnham, Optimizing phase imaging via dynamic force curves, Surf. Sci. 460 (2000) 292–300.

[16] B. Anczykowski, D. Krüger, H. Fuchs, Cantilever dynamics in quasinoncontact force microscopy: spectroscopic aspects, Phys. Rev. B 53 (1996) 15485–15488.

[17] D. Krüger, B. Anczykowski, H. Fuchs, Physical properties of dynamic force microscopies in contact and noncontact operation, Ann. Phys. 6 (1997) 341–363.

[18] B. Anczykowski, D. Krüger, K.L. Babcock, H. Fuchs, Basic properties of dynamic force spectroscopy with the scanning force microscope in experiment and simulation, Ultramicroscopy 66 (1996) 251–259.

[19] J. Tamayo, R. García, Effects of elastic and inelastic interactions on phase contrast images in tapping mode scanning force microscopy, Appl. Phys. Lett. 71 (1997) 2394–2396.

[20] J. Tamayo, R. García, Deformation, contact time, and phase contrast in tapping mode scanning force microscopy, Langmuir 12 (1996) 4430–4435.

[21] M.-H. Whangbo, S.N. Magonov, H. Bengel, Tip-sample force interactions and surface stiffness in scanning probe microscopy, Probe Microsc. 1 (1997) 23–42.

[22] S.N. Magonov, J. Cleveland, V. Elings, D. Denley, M.-H. Whangbo, Tapping-mode atomic force microscopy study of the near surface composition of a styrene–butadiene–styrene triblock copolymer film, Surf. Sci. 389 (1997) 201–211.

[23] S.N. Magonov, V. Elings, M.-H. Whangbo, Phase imaging and stiffness in tapping-mode atomic force microscopy, Surf. Sci. 375 (1997) L385–L391.

[24] J.P. Spatz, S. Sheiko, M. Moeller, R.G. Winkler, P. Reineker, O. Marti, Tapping scanning force microscopy in air— theory and experiment, Langmuir 13 (1997) 4699–4703.

[25] R.G. Winkler, J.P. Spatz, S. Sheiko, M. Moeller, P. Reineker, O. Marti, Imaging material properties by resonant tapping-force microscopy: a model investigation, Phys. Rev. B: Condens. Matter 54 (1996) 8908–8912.

[26] J.P. Spatz, S. Sheiko, M. Moeller, Substrate-induced lateral micro-phase separation of a diblock copolymer, Adv. Mater. (Weinheim, Germany) 8 (1996) 513–517.

[27] A. Noy, C.H. Sanders, D.V. Vezenov, S.S. Wong, C.M. Lieber, Chemically-sensitive imaging in tapping mode by chemical force microscopy: relationship between phase lag and adhesion, Langmuir 14 (1998) 1508–1511.

[28] A. Noy, D.V. Vezenov, C.M. Lieber, Chemical force microscopy, Annu. Rev. Mater. Sci. 27 (1997) 381–421.

[29] S.S. Wong, A.T. Woolley, E. Joselevich, C.M. Lieber, Functionalization of carbon nanotube AFM probes using tip-activated gases, Chem. Phys. Lett. 306 (1999) 219–225.

[30] S.S. Wong, E. Joselevich, A.T. Woolley, C.L. Cheung, C.M. Lieber, Covalently functionalized nanotubes as nanometer-sized probes in chemistry and biology, Nature (London) 394 (1998) 52–55.

[31] K. Feldman, G. Hahner, N.D. Spencer, Surface nanochemical studies of polymers and other organic surfaces by scanning force microscopy, ACS Symp. Ser. 741 (2000) 272–283.

[32] S. Brunner, W.R. Caseri, U.W. Suter, G. Haehner, D. Brovelli, N.D. Spencer, Preparation and characterization of ultrathin layers of substituted oligo- and Poly(*p*-phenylene)s and mixed layers with octadecanethiol on gold and copper, Langmuir 15 (1999) 6333–6342.

[33] A. Marti, G. Haehner, N.D. Spencer, Sensitivity of frictional forces to pH on a nanometer scale: a lateral force microscopy study, Langmuir 11 (1995) 4632–4635.

[34] A. Lio, C. Morant, D.F. Ogletree, M. Salmeron, Atomic force microscopy study of the pressure-dependent structural and frictional properties of *n*-alkanethiols on gold, J. Phys. Chem. B 101 (1997) 4767–4773.

[35] A. Lio, D.H. Charych, M. Salmeron, Comparative atomic force microscopy study of the chain length dependence of frictional properties of alkanethiols on gold and alkylsilanes on mica, J. Phys. Chem. B 101 (1997) 3800–3805.

[36] M. Salmeron, Observing friction at work, Chemtech 28 (1998) 17–23.

[37] X. Xiao, J. Hu, D.H. Charych, M. Salmeron, Chain length dependence of the frictional properties of alkylsilane molecules self-assembled on mica studied by atomic force microscopy, Langmuir 12 (1996) 235–237.

[38] M. Utriainen, A. Leijala, L. Niinistö, R. Matero, Chemical imaging of patterned inorganic thin-film structures by lateral force microscopy, Anal. Chem. 71 (1999) 2452–2458.

[39] G. Bar, R. Brandsch, M.-H. Whangbo, Effect of visco-elastic properties of polymers on the phase shift in tapping mode atomic force microscopy, Langmuir 14 (1998) 7343–7347.

[40] G. Bar, R. Brandsch, M.-H. Whangbo, Effect of tip sharpness on the relative contributions of attractive and repulsive forces in the phase imaging of tapping mode atomic force microscopy, Surf. Sci. Lett. 422 (1999) L192–L199.

[41] X. Chen, M.C. Davies, C.J. Roberts, S.J.B. Tendler, P.M. Williams, J. Davies, A.C. Dawkes, J.C. Edwards, Interpretation of tapping mode atomic force microscopy data using amplitude-phase-distance measurements, Ultramicroscopy 75 (1998) 171–181.

[42] B.B. Sauer, R.S. McLean, R.R. Thompson, Tapping mode AFM studies of nano-phases on fluorine-containing polyester coatings and octadecyltrichlorosilane monolayers, Langmuir 14 (1998) 3045–3051.

[43] R. Höper, T. Gesang, W. Possart, O.-D. Hennemann, S. Boseck, Imaging elastic properties with an atomic force microscope operating in tapping mode, Ultramicroscopy 60 (1995) 17–24.

[44] S.J.T. Van Noort, K.O. Van der Werf, B.G. De Grooth, N.F. Van Hulst, J. Greve, Height anomalies in tapping mode atomic force microscopy in air caused by adhesion, Ultramicroscopy 69 (1997) 117–127.

[45] S. Bardon, M.P. Valignat, A.M. Cazabat, Study of liquid crystal prewetting films by atomic force microscopy in tapping mode, Langmuir 14 (1998) 2916–2924.

[46] H. Brunner, T. Vallant, U. Mayer, H. Hoffmann, Stepwise growth of ultrathin SiO_x films on Si(1 0 0) surfaces through sequential adsorption/oxidation cycles of alkylsiloxane monolayers, Langmuir 12 (1996) 4614–4617.

[47] A. Omoike, G. Chen, G.W. Van Loon, J.H. Horton, Investigation of the surface properties of solid-phase hydrous aluminum oxide species in simulated wastewater using atomic force microscopy, Langmuir 14 (1998) 4371–4376.

[48] M.O. Finot, M.T. McDermott, High-resolution chemical mapping of surface bound functional groups with tapping-mode scanning force microscopy, J. Am. Chem. Soc. 119 (1997) 8564–8565.

[49] S.R. Wasserman, Y.-T. Tao, G.M. Whitesides, Structure and reactivity of alkylsiloxane monolayers formed by reaction of alkyltrichlorosilane on silicon substrates, Langmuir 5 (1989) 1074–1087.

[50] G. Bar, S. Rubin, A.N. Parikh, B.I. Swanson, T.A. Zawodzinski Jr., M.-H. Whangbo, Scanning force microscopy study of patterned monolayers of alkanethiols on gold. Importance of tip-sample contact area in interpreting force modulation and friction force microscopy images, Langmuir 13 (1997) 373–377.

[51] T. Vallant, H. Brunner, U. Mayer, H. Hoffmann, Investigation of formation and structure of self-assembled alkylsiloxane

monolayers on silicon using in-situ ATR-infrared spectroscopy, Langmuir 15 (1999) 5339–5346.
[52] T. Kajiyama, K. Tanaka, S.-R. Ge, A. Takahara, Morphology and mechanical properties of polymer surfaces via scanning force microscopy, Prog. Surf. Sci. 52 (1996) 1–52.
[53] S.P. Jarvis, T.P. Weihs, A. Oral, J.B. Pethica, Mechanics of contacts at less than 100 Å scale: indentation and AFM, Mater. Res. Soc. Symp. Proc. 308 (1993) 127– 132.
[54] S.P. Jarvis, A. Oral, T.P. Weihs, J.B. Pethica, A novel force microscope and point contact probe, Rev. Sci. Instrum. 64 (1993) 3515–3520.
[55] A. Takahara, K. Kojio, S.-R. Ge, T. Kajiyama, Scanning force microscopic studies of surface structure and protein adsorption behavior of organosilane monolayers, J. Vac. Sci. Technol. A 14 (1996) 1747–1754.
[56] T. Komeda, K. Namba, Y. Nishioka, Self-assembled-monolayer film islands as a self-patterned mask for SiO_2 thickness measurement with atomic force microscopy, Appl. Phys. Lett. 70 (1997) 3398–3400.
[57] M.J. Lercel, R.C. Tiberio, P.F. Chapman, H.G. Craighead, C.W. Sheen, A.N. Parikh, D.L. Allara, Self-assembled monolayer electron-beam resists on gallium arsenide and silica, J. Vac. Sci. Technol. B 11 (1993) 2823–2828.
[58] B. Anczykowski, B. Gotsmann, H. Fuchs, J.P. Cleveland, V.B. Elings, How to measure energy dissipation in dynamic mode atomic force microscopy, Appl. Surf. Sci. 140 (1999) 376–382.